Modeling Transmission Lines on Silicon in the Frequency and Time Domains from S-Parameters

Svetlana C. Sejas-García, *Student Member, IEEE*, Reydezel Torres-Torres, *Member, IEEE*, and Roberto S. Murphy-Arteaga, *Senior Member, IEEE*

***Abstract*—This brief presents the full characterization and modeling of uniform transmission lines on silicon. It includes the implementation of equivalent circuit models in both the frequency and time domains to perform accurate and causal simulations up to 30 GHz and for rise times in the order of picoseconds, respectively. These models can be directly implemented in SPICE-like simulators to obtain fast and physically based results when working on RFCMOS.**

***Index Terms*—CPW, skin effect, transmission-line loss.**

I. Introduction

Currently, CMOS technologies are used at microwave frequencies. In this case, the losses occurring at the substrate impact the integrity of signals propagating through IC interconnects. For this reason, many papers that analyze interconnects as transmission lines (TLs) on lossy semiconductor substrates have been presented using data in the frequency (f) domain [1]–[3]. However, these proposals either require precise knowledge of the TL geometry and material properties [1] or involve curve fitting at frequencies where the experimental data typically present considerable noise [2]. Moreover, the f-dependent model parameters used in these proposals complicate time (t)-domain simulations in SPICE-like tools.

Although there are approaches for modeling TLs in the t domain, these use Fourier analysis that requires special considerations to be implemented in circuit simulators [3], are limited in bandwidth [4], or require optimization routines to determine the model parameters [5]. In order to overcome the drawbacks of previous approaches, this brief presents a method to characterize and model TLs on silicon, which is based on processing per-unit-length propagation constant $(\gamma = \alpha + j\beta)$ and characteristic impedance (Z_0) data. Once the TLs are fully characterized in the f domain, f-dependent effects are modeled using a combination of f-independent circuit elements that allow for the performance of simulations in the t domain in a simple and direct way. The proposed modeling and parameter-extraction strategy are verified up to 30 GHz, and causal results are obtained in the time domain for a rise time (t_r) as small as 12 ps.

Manuscript received November 4, 2011; revised January 9, 2012; accepted February 24, 2012. Date of publication April 13, 2012; date of current version May 23, 2012. This work was supported by CONACyT, Mexico through grant 83774-Y and scholarship 213385. The review of this brief was arranged by Editor D. Esseni.

The authors are with the Department of Electronics, Instituto Nacional de Astrofísica, Óptica y Electrónica, Puebla 72840, Mexico (e-mail: carsof@inaoep.mx).

Color versions of one or more of the figures in this brief are available online at http://ieeexplore.ieee.org.

Digital Object Identifier 10.1109/TED.2012.2189774

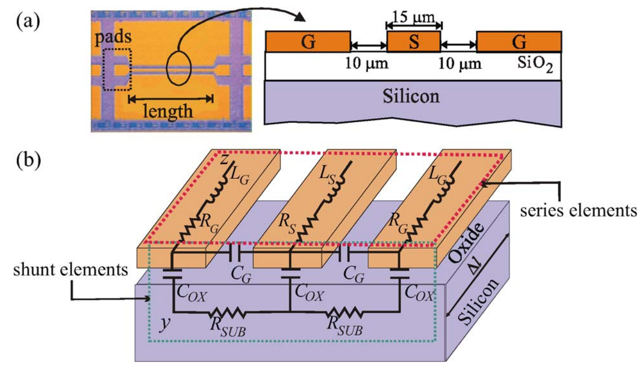

Fig. 1. Sketch of the fabricated CPWs: (a) micrograph and cross section detailing dimensions and (b) equivalent circuit model for a homogeneous section of a line with length Δl.

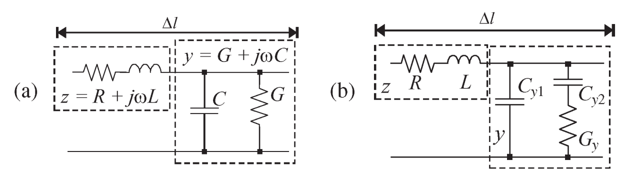

Fig. 2. Models for representing a CPW: (a) conventional model and (b) alternative representation where y is modeled with elements independent of f.

II. Prototypes and Measurements

In order to show the development and verification of the proposal, CPWs of several lengths (from 250 to 6400 μm) were fabricated on an RFCMOS process. These TLs were formed with aluminum on field oxide grown on a p-type silicon substrate with a 20-$\Omega \cdot$cm resistivity. The dimensions of the structures and an equivalent circuit model for a section with length Δl are depicted in Fig. 1(a) and (b), respectively. Notice that pads are included to measure S-parameters using ground–signal–ground (GSG) probes with a 150-μm pitch. For this purpose, a vector-network-analyzer setup was calibrated by applying an off-wafer line–reflect–match algorithm and an impedance standard substrate. Once the CPWs were measured, γ and Z_0 were obtained as in [6] to remove the pad parasitics from the measurements. Subsequently, the experimental data for the per-unit-length $RLGC$ elements in the conventional model of a TL in Fig. 2(a) were calculated as $R = \mathrm{Re}(\gamma Z_0)$, $L = \mathrm{Im}(\gamma Z_0)/2\pi f$, $G = \mathrm{Re}(\gamma/Z_0)$, and $C = \mathrm{Im}(\gamma/Z_0)/2\pi f$.

0018-9383/$31.00 © 2012 IEEE

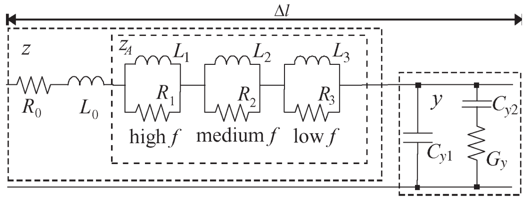

Fig. 3. TL model representing R and L using f-independent elements.

III. Model Implementation

In Fig. 1(b), several capacitances and conductances represent the shunt elements in a CPW on silicon. However, assuming symmetry with respect to the signal trace, this model can be simplified to the alternative form shown in Fig. 2(b), which is similar to that used for GSG probing pads [6]. The advantage of this model, when compared with the model in Fig. 2(a), is the fact that C_{y1}, C_{y2}, and G_y are independent of f at microwave frequencies [2], simplifying the analysis as shown hereafter.

The series elements R and L are strongly impacted by the f-dependent distribution of the current on the cross section of the metal lines, which is associated with the skin effect. In this case, an appropriate representation is achieved using [3]

$$R = R_0 + K_R\sqrt{f} \tag{1}$$
$$L = L_0 + \frac{K_R}{2\pi\sqrt{f}}. \tag{2}$$

Since R_0, K_R, and L_0 are constant in f, simple data regressions can be used to implement (1) and (2) for the fabricated CPWs.

For the case of the shunt elements, G_y, C_{y1}, and C_{y2} are related to G and C in the conventional model through

$$G = AG_yC_{y2}^2(2\pi f)^2 \tag{3}$$
$$C = C_{y1} + A \tag{4}$$

with $A = 1/(G_y^2 + C_{y2}^2(2\pi f)^2)$. In this case, the f-independent C_{y1}, C_{y2}, and G_y are obtained as for GSG probing pads [6].

Even though (1)–(4) allow to accurately reproduce the experimental $RLGC$ parameters, the terms including K_R in (1) and (2) do not present a circuit equivalence using f-independent elements, which complicates the corresponding implementation in SPICE-like tools for performing t-domain simulations. Hence, several approaches to approximately represent the dependence of R and L on f using equivalent circuits [4], [5] are available but require optimization techniques to obtain the corresponding parameters. Thus, the parameter-extraction method proposed here is based on a systematic procedure that involves simple data regressions, which allows a circuit-model implementation in a direct and simple way. This is explained hereafter.

The selected model to represent R and L is shown in Fig. 3, where the f-dependent terms in (1) and (2) are approximated through the series connection of several blocks of resistors (R_i) and inductors (L_i) in parallel. In this case, the number of required blocks increases as the range of frequencies to be considered becomes wider. For the fabricated CPWs, three blocks were used, achieving good accuracy up to 30 GHz. More details on the determination of the number of blocks needed for higher frequencies are given hereafter.

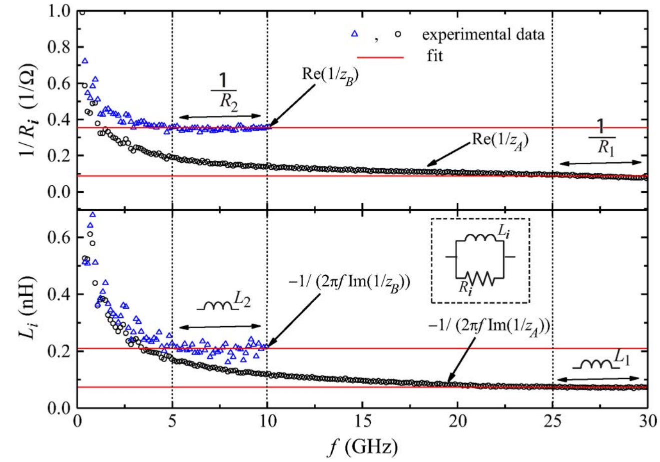

Fig. 4. Extraction of the inductances and resistances for the blocks representing the f-dependent terms of z at medium and high frequencies.

The parameter extraction starts removing the f-independent terms R_0 and L_0 from the series impedance of the CPW (i.e., z), resulting in the following impedance:

$$z_A = z - (R_0 + j\omega L_0) = (R - R_0) + j\omega(L - L_0) \tag{5}$$

which includes only the f-dependent terms in (1) and (2). In this case, each one of the blocks in Fig. 3 allows to represent z_A in different f ranges.

The following step consists of determining the resistance and inductance associated with each block, starting with R_1 and L_1. Hence, assuming that the parallel connection of these elements approximately represents z_A at high frequencies, the following approximation can be used:

$$\frac{1}{z_A} \approx \frac{1}{R_1} - \frac{j}{2\pi f L_1} \quad \text{for} \quad f \gg 0. \tag{6}$$

In practice, the experimental $\mathrm{Re}(1/z_A)$ approaches a constant value at high frequencies, which allows to determine $1/R_1$, as shown in Fig. 4. Likewise, this figure shows the value determined for L_1 when plotting $-1/2\pi f\mathrm{Im}(1/z_A)$ versus f.

Afterward, the effect of R_1 and L_1 is removed from z_A, resulting in the following impedance:

$$z_B = z_A - (R_1 + j2\pi f L_1) \tag{7}$$

which represents the f-dependent terms in (1) and (2) at medium and low frequencies. Thus, when plotting $1/\mathrm{Re}(z_B)$ versus f, a constant value is observed at medium frequencies, which correspond to those just below the range where the effect of R_1 and L_1 is dominant in the total f-dependent series impedance. From this constant value, $1/R_2$ is determined. Similarly, L_2 is obtained when plotting $-1/2\pi f\mathrm{Im}(1/z_B)$ versus f at these frequencies. These extractions are shown in Fig. 4.

A third impedance z_C can be defined to represent the f-dependent terms of the series impedance at low frequencies. In fact, subsequent impedances can be defined to extract the parameters of additional blocks until the whole f range of interest is covered. Fig. 5 shows a model–experiment confrontation

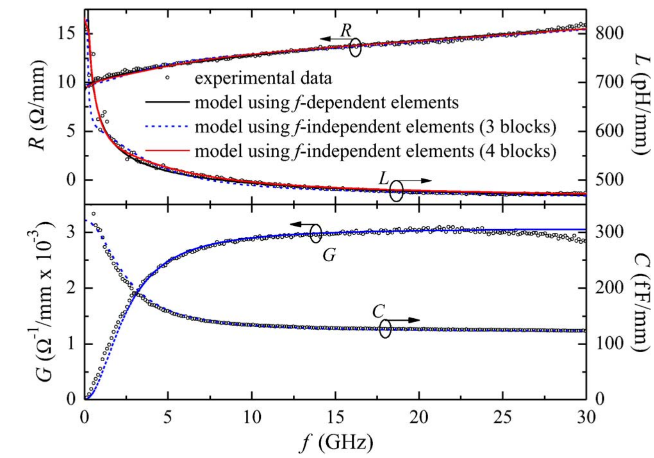

Fig. 5. Curves showing the model–experiment correlation for R, L, C, and G.

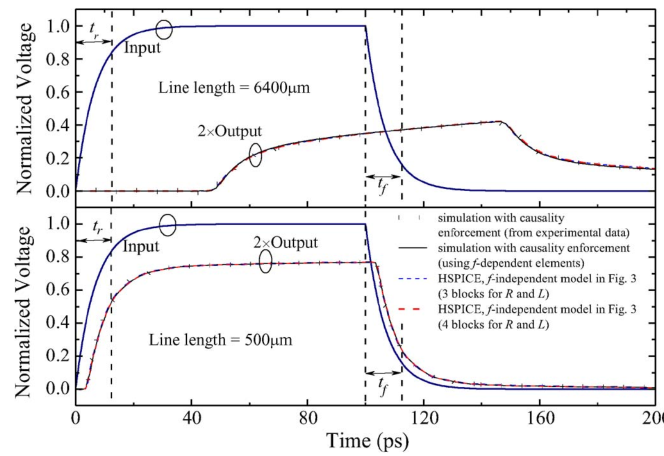

Fig. 6. Waveforms in the t domain obtained using the model in Fig. 3 and using commercial simulators applying iFFT and a causality correction.

in the f domain when applying (1)–(4) and when using the circuit in Fig. 3 in HSPICE after obtaining the corresponding parameters with the proposed method.

For assessing the accuracy of these models, the feature selective validation (FSV) can be applied [7], [8]. In this case, the total amplitude difference measure (ADMt) can be computed, which is a figure that provides the goodness of fit between two data sets. In fact, when ADMt < 0.1, a model is considered as excellent [7]. Regarding the models in Fig. 5 for R, for the one that directly uses (1)–(4), ADMt $= 0.034$, whereas for the f-independent model in Fig. 3, ADM $= 0.081$. Thus, both of them are considered as excellent, and similar results are obtained for L. Notice also that Fig. 5 includes the curve corresponding to a simulation after including a fourth block. Even though more accuracy (e.g., ADM $= 0.035$ for R) is obtained, considering a tradeoff between accuracy and simulation time might be necessary for implementing the model, particularly for circuits including many interconnects.

IV. Results in the Time Domain

A common practice for analyzing the response of a TL in the t domain is obtaining the corresponding transfer function from f-domain data using an inverse fast Fourier transform (iFFT). For the TLs analyzed here, these f-domain data can be defined using either of the following: 1) experimental S-parameters or 2) the circuit shown in Fig. 2(b). For the latter case, basic TL-theory concepts are used to obtain the minimum number of $RLGC$ blocks in cascade for representing a line of a given length.

In accordance to [9], it can be demonstrated that using data up to 30 GHz presenting f steps of 150 MHz allows for the representation of signals with t_r as small as 12 ps propagating in lines with a delay time as long as 6.6 ns. Following these guidelines, a model to perform t-domain simulations was implemented in Agilent's ADS simulator directly using the experimental S-parameters of the CPWs and f-domain data generated using the model in Fig. 2(b). It is important to point out that this simulator applies a causality enforcement algorithm to obtain realistic results.

Even though the previously described simulations allow us to obtain causal results, a model to directly perform t-domain simulations using a circuit containing only f-independent elements is desirable. This is because this type of circuit is compatible with SPICE-like tools. Thus, a model based on the circuit shown in Fig. 3 was implemented in HSPICE to perform simulations that can be compared to the ones obtained using iFFT. As noticed in Fig. 6, the waveforms at the output of two lines presenting different lengths were obtained when a pulse voltage with $t_r = 12$ ps was applied at the input terminals. After performing an FSV analysis, it is observed that excellent agreement between the obtained waveforms with the model in Fig. 3 and when using the simulations involving iFFT of f-domain data is achieved (i.e., ADMt < 0.1 in all cases). The agreement is due to the accurate modeling of the $RLGC$ elements implementing the model in Fig. 3 using the proposed extraction method up to 30 GHz.

V. Conclusion

Excellent model–experiment correlations have been obtained in the frequency domain up to 30 GHz when using a SPICE-compatible equivalent circuit. The accuracy is due to a simple extraction methodology that allows to obtain the model parameters in a simple and direct way. Moreover, the accuracy of the model can be extended to higher frequencies when including more elements in the equivalent circuit and performing subsequent extractions using the proposed methodology. It has been verified that this model also allows to obtain waveforms in the time domain that accurately reproduce those obtained with commercial software that applies frequency-to-time-domain-transform techniques. Moreover, since this methodology uses experimental data involving γ and Z_0, all the physical effects influencing the electrical characteristics of the TLs are adequately taken into consideration, including the substrate losses occurring in CMOS technologies. Thus, the proposed procedure can be applied to any set of homogeneous TLs with the same cross section and operating in single propagation mode provided that the corresponding γ and Z_0 are known.

ACKNOWLEDGMENT

The authors would like to thank IMEC for supplying the test structures.

REFERENCES

[1] C. Chen, R. Wang, Y. Su, and T. Hsueh, "A nanocrystalline silicon surface-passivation layer on an HR-Si substrate for RFICs," *IEEE Electron Device Lett.*, vol. 32, no. 3, pp. 369–371, Mar. 2011.

[2] L. Tran, D. Pasquet, E. Bourdel, and S. Quintanel, "CAD-oriented model of a coplanar line on a silicon substrate including eddy-current effects and skin effect," *IEEE Trans. Microw. Theory Tech.*, vol. 56, no. 3, pp. 663–670, Mar. 2008.

[3] J. Zhang, J. L. Drewniak, D. J. Pommerenke, M. Y. Koledintseva, R. E. DuBroff, W. Cheng, Z. Yang, Q. B. Chen, and A. Orlandi, "Causal RLGC(f) models for transmission lines from measured S-parameters," *IEEE Trans. Electromagn. Compat.*, vol. 52, no. 1, pp. 189–198, Feb. 2010.

[4] H. Kim and Y. Eo, "High-frequency-measurement-based frequency-variant transmission line characterization and circuit modeling for accurate signal integrity verification," in *Proc. 8th Int. Symp. Quality Electron. Des.*, Mar. 2007, pp. 507–512.

[5] A. Schellmanns, J. Keradec, and J. Schanen, "Electrical equivalent circuit for frequency dependant impedance: Minimum lumped elements for a given precision," in *Proc. Ind. App. Conf.*, Oct. 2000, vol. 5, pp. 3105–3115.

[6] R. Torres-Torres, R. Venegas, and S. Decoutere, "Transmission line characterization on silicon considering arbitrary distribution of the series and shunt pad parasitics," *Solid-State Electron.*, vol. 54, no. 3, pp. 235–242, Mar. 2010.

[7] A. P. Duffy, A. J. M. Martin, A. Orlandi, G. Antonini, T. M. Benson, and M. S. Woolfson, "Feature selective validation (FSV) for validation of computational electromagnetics (CEM). Part I—The FSV method," *IEEE Trans. Electromagn. Compat.*, vol. 48, no. 3, pp. 449–459, Aug. 2006.

[8] A. Orlandi, A. P. Duffy, B. Archambeault, G. Antonini, D. E. Coleby, and S. Connor, "Feature selective validation (FSV) for validation of computational electromagnetics (CEM). Part II—Assessment of FSV performance," *IEEE Trans. Electromagn. Compat.*, vol. 48, no. 3, pp. 460–467, Aug. 2006.

[9] D. Kaller, C. Schuster, Y. Kwark, D. Altabella, B. Truong, Z. Chen, A. Haridass, and E. Klink, "Using S-parameters successfully in time domain link simulations," in *Proc. 14th IEEE EPEPS*, Oct. 2005, pp. 95–98.

Svetlana C. Sejas-García (S'09) was born in Puebla, Mexico. She received the B.S. degree in electronics from the Benemérita Universidad Autónoma de Puebla, Puebla, in 2005 and the M.S. degree in electronics from INAOE, Puebla, in 2009, where she is currently working toward the Ph.D. degree by researching the effects occurring in complex chip-to-chip communication channels.

In 2008, she was an Intern with Intel Laboratories, Mexico, working on the development of models for high-speed interconnects.

Reydezel Torres-Torres (S'01–M'06) received the Ph.D. degree from INAOE, Puebla, Mexico.

He has worked for Intel Laboratories, Mexico, and IMEC, Belgium. He is a Senior Researcher with the Microwave Research Group, INAOE. He has authored more than 30 journal and conference papers and directed three Ph.D. and six M.S. theses, all in high-frequency characterization and modeling of materials, interconnects, and devices for microwave applications.

Roberto S. Murphy-Arteaga (SM'00) received the B.S. degree in physics from Saint John's University, Collegeville, MN, and the M.Sc. and Ph.D. degrees from INAOE, Puebla, Mexico.

Since 1988, he has been teaching graduate courses at INAOE, totaling over 100 taught undergraduate and graduate courses, where he is currently a Senior Researcher with the Microelectronics Laboratory and the Academic Dean. He has given over 70 talks at scientific conferences and directed 6 Ph.D., 12 M.Sc., and 2 B.Sc. theses. He has published more than 100 articles in scientific journals, conference proceedings, and newspapers and is the author of a textbook on electromagnetic theory. His research interests are the physics, modeling, and characterization of the MOS transistor and passive components for high-frequency applications, particularly for CMOS wireless circuits, and antenna design.

Dr. Murphy-Arteaga is the Chairman of ISTEC's Board of Directors, a member of the Mexican Academy of Sciences, and a member of the Mexican National System of Researchers (SNI).